AMERICAN JOURNAL OF PHYSICAL ANTHROPOLOGY 109:89–110 (1999)

Morphological and Taxonomic Affinities of the Olduvai Ulna (OH 36)

LESLIE C. AIELLO,[1]* BERNARD WOOD,[2]
CATHY KEY,[1] AND MARK LEWIS[1]
[1]*Department of Anthropology, University College London, London WC1 6BT, UK*
[2]*Department of Anthropology, George Washington University, Washington, DC 20052*

KEY WORDS fossil hominin; Olduvai; ulna; OH 36; *Homo erectus; Paranthropus boisei;* human evolution; bootstrapping; species recognition

ABSTRACT The OH 36 ulna derives from Upper Bed II in the Olduvai Gorge, and is dated to circa 1.1–1.2 Myr. Multivariate analyses incorporating data from samples of modern humans, common and pygmy chimpanzees, gorillas, orangutans, and two other early hominin ulnae, Omo L40-19 and KNM-BK 66, suggest that OH 36 belonged to an individual with powerful forearms consistent with a locomotor repertoire that included arboreal locomotion. However, there is no compelling evidence that it made regular use of its forelimbs as supports when travelling on the ground. When compared with levels of intra- and intertaxon size and shape variation in the comparative sample (humans, chimpanzees, gorillas), the differences between OH 36, KNM-BK 66, and Omo L40-19 are compatible with OH 36 differing from the other two fossil hominin ulnae to the extent that modern humans differ from modern great apes. KNM-BK 66 and Omo L40-19 differ from each other in overall size and shape only to the degree that would be expected within any of the individual modern comparative samples.

Based on these analyses, there is no evidence to support the hypothesis that OH 36 and Omo L40-19 belong to the same species of fossil hominin, or to two species that shared a similar forelimb locomotor repertoire. We suggest that OH 36 has the greater claim to be assigned to *Paranthropus boisei*, and we recommend that for the time being the latter be referred to the tribe Hominini gen. et sp. indet. The surprising result of these analyses is the overall size and shape similarity between Omo L40-19 and KNM-BK 66, two fossils that are separated in time by more than 1.5 million years, and which have traditionally been assumed to represent hominin species with quite different locomotor patterns. Am J Phys Anthropol 109:89–110, 1999.

An almost complete hominin right ulna (Olduvai Hominid 36, or OH 36) was recovered in situ at site SC in Upper Bed II, Olduvai Gorge, Tanzania by M. Mutala in 1970. Although OH 36 has yet to be formally described, at various times it has been assigned to the hypodigms of *Homo erectus* (Leakey, 1978; Day, 1986; Tobias, 1991) and *Australopithecus boisei* (hereafter referred to as *Paranthropus boisei*) (Walker and Leakey, 1993).

Relatively few hominin fossils derive from Upper Bed II. The only other hominin remains to be recovered from site SC (OH 38, comprising a molar and two incisors) have

Grant sponsor: Leverhulme Trust; Grant numbers: F 134 BB, A 953767; Grant sponsor: Henry R. Luce Foundation.

*Correspondence to: Leslie C. Aiello, Department of Anthropology, University College London, London WC1 6BT, UK. E-mail: L.Aiello@ucl.ac.uk

Received 29 May 1998; accepted 11 February 1999.

been referred to cf. *P. boisei* (Leakey, 1978). A deciduous molar and canine, OH 3, recovered from Upper Bed II in 1955 at site BK, have also been referred to cf. *P. boisei* (Leakey, 1978). The best known hominin recovered from Upper Bed II is the calvaria, OH 9, which was discovered at site LLK in 1960. This was referred to *Homo erectus* (Leakey, 1961), and this assignment has since received wide support (e.g., Rightmire, 1979; Wood, 1991).

The OH 36 ulna was found at the top of Upper Bed II, above the uppermost tuff (IID). Unfortunately this tuff has produced no reliable radiometric dates. The age of OH 36 has been estimated using the relative thickness of the strata between the top of the Lemuta Member, which lies lower in Bed II and is dated at c. 1.6 Myr, and Tuff IVB in Bed IV, which apparently marks the Brunhes-Matuyama boundary (0.7 Myr) (Hay, 1976). The age estimated for Upper Bed II of c. 1.15 Myr corresponds with a major phase of Rift Valley faulting at 1.15–1.2 Myr that most probably relates to the disconformity between Beds II and III (Hay, 1976). If an age c. 1.15 Myr is accepted for the top of Bed II, and if OH 36 and the teeth from SC and BK were to belong to *P. boisei*, then this material would be among the most recent fossil evidence of *P. boisei*, postdating conspecific evidence from the Omo region (Wood et al., 1994) and the cranial evidence known from Chesowanja (Carney et al., 1971; Gowlett et al., 1981).

Recent work on comparative forelimb morphology has shown that, despite considerable intraspecific variability, the ulna can be used to distinguish between archaic and modern humans (Trinkaus, 1983, 1989, 1992; Churchill et al., 1996; Pearson and Grine, 1996). The best-preserved ulna in the early hominin fossil record is the almost complete Omo L40-19 ulna recovered from Member E of the Omo Shungura Formation. This specimen is dated at c. 2.3 Myr (Feibel et al., 1989) and has been assigned to *P. boisei* (Howell and Wood, 1974; McHenry et al., 1976; Aiello and Dean, 1990), or to *Paranthropus* cf. *aethiopicus/boisei* (Howell et al., 1987). Previous analyses have concluded that Omo L40-19 resembles the living apes, and particularly chimpanzees, in some features (e.g., overall length relative to length of the trochlea, degree of shaft curvature, and absence of a marked interosseous crest) (Howell and Wood, 1974; McHenry et al., 1976; Feldesman, 1979), while in other features (e.g., the shortness overall and the anteroposterior depth of the olecranon) it is unique (McHenry et al., 1976; Howell et al., 1987).

Omo L40-19 is larger and generally more robust than KNM-BK 66 from the Kapthurin Formation, Baringo, Kenya (dated at between 0.24–0.73 Myr, probably c. 0.6–0.7 Myr), which is the only well-preserved adult ulna that is presumed to belong to an adult *H. erectus* (Senut, 1981; Solan and Day, 1992). Similarities between the Baringo ulna and later archaic *H. sapiens* ulnae have recently been emphasized by Churchill et al. (1996) and Pearson and Grine (1996), and KNM-BK 66 has also been described as being "very similar" to KNM-WT 15000 BP and BZ, the ulnae belonging to the Nariokotome early African *Homo erectus*, or *H. ergaster*, skeleton (Walker and Leakey, 1993, p 131).

In this paper, we provide a formal description of the OH 36 ulna, reconstruct its length, and then compare it with modern hominoid ulnae, with KNM-BK 66 and Omo L40-19, and with other more fragmentary Pliocene and Pleistocene fossil hominin ulnae from southern Africa. The purposes of the study are 1) to determine the similarities and differences between the Olduvai ulna and the various comparators, and 2) to assess the degree of similarity between OH 36 and contemporary fossil hominin ulnae which have been assigned to *P. boisei* and *H. erectus*. The results of these two studies will then be integrated to form the basis of a taxonomic assessment of OH 36.

MORPHOLOGICAL DESCRIPTION

The specimen consists of a nearly complete right ulna comprising three conjoined fragments (Fig. 1). The well-marked muscle attachments and the evident fusion of the secondary centers suggest that the bone is of an adult. The distal fracture surface is just distal to the pronator crest and close to the neck. The total length of the preserved specimen is 264 mm. Apart from damage to the

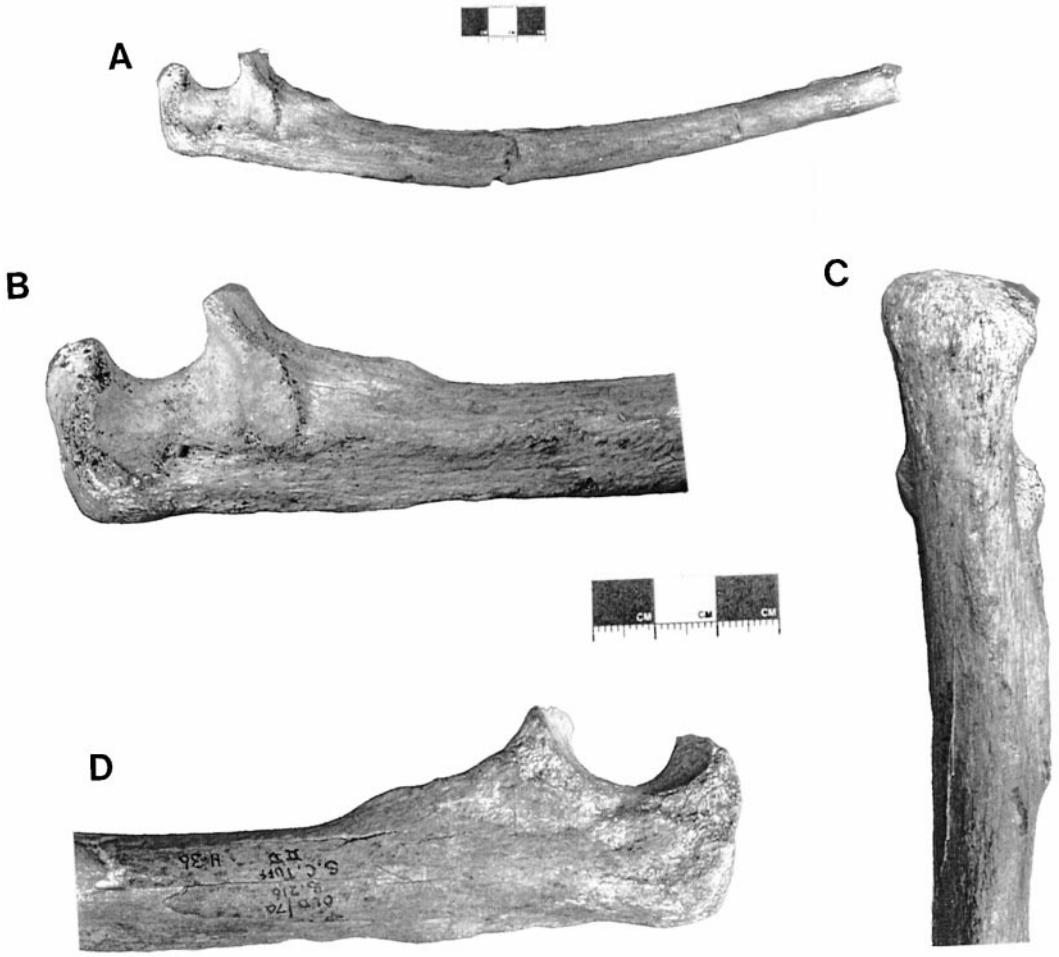

Fig. 1. The OH 36 ulna. **A:** Lateral view. **B:** Lateral view of proximal end. **C:** Dorsal view of proximal end. **D:** Medial view of proximal end.

medial surfaces of the olecranon and coronoid processes, the absence of a wedge of bone at the proximal end of the middle of the three conjoined fragments, and the loss of surface bone at some sites on the shaft, the specimen is well-preserved.

The shaft is curved in the sagittal plane, concave anteriorly. The markings on the shaft vary in their development. The interosseous crest is weakly developed (but surface bone is missing for some of its likely course), while the supinator crest is strongly marked. The posterior border is ridge-like proximally, but distally it is much less well-delineated. It is sinuous, convex laterally proximally, and concave laterally distally. The medial surface of the shaft is featureless. Anteriorly, the ulnar tuberosity is well-developed and has a 10-mm-long, linear, pit-like depression running along its center towards the distal end, in line with the long axis of the shaft.

The olecranon projects posteriorly in relation to the proximal ulna shaft, and this is an expression of the relatively large attachment for triceps. The proximal border of the olecranon forms an angle of approximately 100° with the posterior border of the ulna shaft. The majority of the surface of the olecranon is smooth, but the roughened area at the base of the process extends onto the posterior aspect of the proximal end of the

ulna shaft, and marks the substantial attachment of the triceps muscle. The coronoid process is damaged where any sublime tubercle would have been. The trochlear notch is oriented somewhat anteroproximally, and its sagittal profile is symmetrical. The undamaged tip of the coronoid process projects 4 mm above the tip of the olecranon. The lateral articular surface of the trochlea is substantially larger than the medial one. They meet at an acute angle at a substantial midline keel. The teardrop-shaped radial notch has its long axis orientated anteroposteriorly. Its surface is smooth and uniformly concave. The 20-mm-long pronator crest is the only notable feature at the distal end of the shaft.

MATERIALS AND METHODS

The extant comparative sample consists of 240 modern human, orangutan, and African ape ulnae. This sample includes two subspecies of gorilla, *Gorilla g. gorilla* and *Gorilla g. graueri*, two subspecies of chimpanzee, *Pan t. troglodytes* and *Pan t. schweinfurthi*, *Pan paniscus*, *Pongo pygmaeus*, and eight population samples of modern humans. Details of this comparative sample are given in Table 1, along with the means and standard deviations for all measurements used in the analysis. The Pliocene and Pleistocene fossil hominin ulnae from East and southern Africa that were included in the study are listed in Table 2, along with the measurements taken on these specimens. All measurements are defined in Table 3 and illustrated in Figure 2. Measurements, to the nearest 0.1 mm, were taken by one of two observers; original fossil specimens were measured unless otherwise indicated.

Interobserver error was tested by comparing the measurements taken by the two observers on 10 ulnae from the Andaman Island sample (Table 3). Error was assessed in two ways: the coefficient of variation and the percentage measurement error. With two exceptions, the percentage measurement error was under 1.00%. The two exceptions were the length to the pronator quadratus crest (PQlength) and curvature cord (CurvCord), which have interobserver errors of 1.12% and 1.25%, respectively (Table 3). Both of the measurements used termini that are sometimes difficult to define. All data were screened for measurement and entry errors.

Three different sets of analyses were performed. The first used multiple regression analysis to reconstruct the length of the OH 36 ulna. The second set used discriminant function analysis to assess the similarities and differences within the extant comparative sample, and between this sample and OH 36, KNM-BK 66, the presumed *H. erectus* ulna from the Kapthurin Formation west of Lake Baringo, and Omo L40-19, the presumed *P. boisei* ulna from the Shungura Formation. We used discriminant function analysis because our experience of applying principal components and average taxonomic distance methods to raw data, or to size-corrected raw data, demonstrated that the methods were unable to capture the relatively subtle differences between fossil ulnae. This resulted in inconsistent results when pairwise comparisons were made between fossil ulnae. The wider implications of our experience for the comparative analysis of isolated fossils are being explored (Aiello et al., unpublished results). The third set of analyses used bootstrapping to ascertain the probability that OH 36 belongs to the same taxon as Omo L40-19 and KNM-BK 66. This is an empirical method of determining the probability of observing the degree of variation observed in that fossil sample in a modern sample (Lockwood et al., 1996). Repeated samples of the same size as the fossil sample are drawn from each of the comparative samples, and the size and shape variation in each of these samples is assessed.

Size and shape for each modern and fossil comparator are based on 19 ulnar measurements indicated in Table 3, using methods that have become standard in human palaeontology (Grine et al., 1993, 1996; Richmond et al., 1993, Richmond and Jungers, 1995; Kramer et al., 1995; Lague and Jungers, 1996). Size dimorphism is the ratio of the geometric mean of one specimen to that of another. The geometric mean is one of the Mosimann family of size variables, and is calculated as the nth root of the product of n measurements. Combined size and shape

TABLE 1. Comparative sample and the means and standard deviations for all measurements used in the analysis[1]

	Length	PQLength	CurvCord	CurvSt	CrestMin	CrestMax	PQMax	PQMin	OlecLt	OlecHt	OlecArt	OlecMax	TrocCord	TrocTv	TrocAp	TrocSt	CorHt	CorBt	PosTub
Gorilla																			
G. gorilla gorilla (20)	352.4	287.1	284.4	13.2	22.4	24.9	15.5	13.9	27.2	30.9	35.2	37.6	28.7	33.9	27.5	14.2	48.9	36.2	48.8
	39.6	35.4	35.8	2.2	3.5	3.9	2.4	2.3	3.6	4.7	5.9	6.4	3.8	5.5	4.6	1.5	6.9	5.9	7.4
G. gorilla graueri (12)	330.6	261.3	269.6	20.0	20.8	24.0	15.6	15.0	21.1	33.8	33.0	35.4	26.8	32.0	26.9	13.5	46.5	37.9	45.1
	36.6	31.5	31.7	4.2	4.0	3.6	2.5	2.8	3.9	8.6	5.3	6.5	3.7	5.5	5.0	1.9	7.1	6.9	7.2
Pan																			
P. paniscus (16)	273.7	218.4	227.3	13.0	14.0	14.1	10.7	9.6	15.9	26.2	20.6	22.2	19.4	15.5	19.0	10.7	32.8	22.8	28.0
	9.5	7.4	9.2	2.0	1.4	1.6	0.6	0.7	1.5	1.7	1.7	1.3	1.4	2.9	1.3	0.7	1.5	1.2	2.9
P. t. schweinfurthii (16)	278.3	224.7	228.8	13.6	16.2	16.7	11.7	11.2	18.3	30.5	22.5	24.3	20.7	16.9	22.4	11.3	36.3	23.4	35.2
	17.9	17.2	15.1	3.1	2.8	3.5	1.7	1.5	2.4	3.2	2.2	2.9	2.5	3.2	2.8	1.4	3.7	2.6	3.5
P. t. troglodytes (20)	280.6	215.0	234.3	14.1	15.5	17.7	12.5	12.4	18.0	30.5	21.9	24.6	21.0	16.5	21.6	11.4	37.5	23.4	36.7
	12.8	16.2	12.0	2.3	2.1	2.2	1.2	1.7	1.7	3.3	1.4	2.1	2.5	1.9	2.2	1.1	2.6	2.5	3.8
Pongo																			
P. pygmaeus (14)	353.2	275.5	294.3	12.2	16.4	20.3	12.5	10.9	18.3	22.6	22.7	24.2	20.6	21.1	18.6	11.5	34.3	29.7	48.2
	30.6	23.9	28.1	2.4	2.6	2.3	1.9	2.0	1.6	2.3	2.5	2.7	3.1	2.6	2.4	1.8	4.8	3.3	6.6
Homo sapiens																			
Dart collection (22)	255.1		210.0	5.4	13.3	15.6	11.7	10.0	18.8	22.0	23.8	24.2	21.6	14.4	16.7	11.4	33.4	23.7	32.9
	19.5		16.4	2.6	1.5	1.6	1.4	1.5	2.3	3.8	2.7	2.4	2.4	1.6	1.5	1.3	3.1	2.6	3.4
Inuit (20)	229.4	186.7	180.2	4.2	11.8	16.1	12.4	9.9	19.5	23.9	24.8	25.4	22.5	16.4	17.7	11.8	34.6	25.5	28.9
	13.9	13.4	12.2	2.1	1.2	1.9	1.4	1.2	1.5	1.8	2.0	2.2	2.2	2.5	1.7	0.9	2.5	2.2	2.3
Terry collection (20)	268.9	219.4	215.2	4.3	13.5	17.2	12.6	10.6	19.9	25.1	26.7	27.1	22.9	15.0	18.2	12.7	36.3	26.8	34.9
	20.4	19.4	16.3	2.1	1.8	2.1	1.5	1.2	2.0	2.7	3.6	3.5	2.8	1.8	1.6	1.5	3.0	3.9	2.5
Romano-British (20)	251.9	190.6	195.1	4.0	14.5	17.1	12.7	12.0	19.4	25.2	24.6	25.6	21.3	16.8	18.5	11.6	35.9	24.7	32.6
	18.4	13.7	15.7	1.7	2.0	1.9	1.6	1.7	2.1	2.3	2.1	2.5	1.8	2.4	1.4	1.7	3.0	3.2	4.3
Spitalfields (20)	231.1	175.1	178.0	4.6	12.6	17.0	12.3	11.2	18.1	23.0	23.4	24.2	19.5	14.7	16.9	11.3	32.9	23.8	29.8
	18.9	14.2	17.8	1.5	2.2	2.3	1.4	1.4	2.2	2.5	3.0	2.9	2.0	2.2	1.4	1.7	3.1	3.2	3.5
Andaman Islanders (10)	236.4	176.8	188.1	5.6	10.3	13.7	9.9	9.3	16.0	20.0	20.1	20.8	19.0	14.4	14.2	9.7	28.2	19.3	27.5
	12.9	8.8	14.2	1.5	0.1	1.7	1.1	1.0	1.1	1.6	2.0	1.9	1.6	1.4	1.3	1.0	2.4	2.1	2.9
Ensay Islanders (20)	248.4	188.7	187.7	3.9	14.0	17.5	13.4	11.2	20.0	24.2	24.9	25.4	21.3	16.6	17.8	12.5	35.5	24.6	29.8
	15.9	14.6	18.0	2.1	2.4	1.8	1.6	1.4	1.5	3.5	2.9	2.9	2.5	3.0	2.4	1.7	4.8	3.9	3.2
Australian Aborigines (10)	266.9	196.3	217.1	6.3	13.4	15.9	11.5	10.5	18.7	24.3	23.4	24.1	20.4	14.1	17.2	11.6	34.1	24.4	29.5
	14.5	8.1	13.8	2.0	2.2	2.3	1.5	1.8	1.8	2.0	1.8	2.0	2.4	2.3	1.4	1.6	3.3	2.8	3.4

[1] Numbers in parentheses following sample designations represent sample sizes. Equal numbers of males and females were measured wherever possible. For each variable for each sample, the upper number represents the sample mean and the lower number the standard deviation. Dart collection, southern African Blacks housed in the Department of Anatomy, University of the Witwatersrand, Johannesburg; Terry collection, North American Blacks housed at the Smithsonian Institution, Washington DC; Inuit, Sadermiut collection in the Canadian Museum of Civilization, Ottawa, Canada. All other human samples as well as those of *Pan troglodytes troglodytes*, *Gorilla gorilla gorilla*, and *Pongo pygmaeus* are housed at the Natural History Museum, London. The remaining ape samples (*Pan troglodytes schweinfurthi*, *Pan paniscus*, and *Gorilla gorilla graueri*) are housed at the Musée royal de l'Afrique centrale, Tervuren, Belgium.

TABLE 2. Early hominin fossil ulnae and measurements[1]

	Length	PQ-Length	Curv-Cord	Curv-St	Crest-Min	Crest-Max	PQ-Max	PQ-Min	Olec-Lt	Olec-Ht	Olec-Art	Olec-Max	Troc-Cord	Troc-Tv	Troc-Ap	Troc-St	Cor-Ht	Cor-Bt	Pos-Tub
KNM-BK 66		245.0	236.0	9.0	12.1	14.8	12.7	8.7	16.0	24.8	22.8	23.8	17.9	18.5	16.5	9.2	27.6	17.9	32.9
OH 36		233.0	220.0	16.0	16.3	17.3	16.0	14.0	21.0	33.0	21.0	25.0	19.0	16.5	23.0	11.2	38.0	22.0	35.0
Omo L40-19 Min	306.0	247.0	253.0	13.0	13.5	20.1	17.1	10.0	20.2	28.2	27.1	29.1	(24.0)	16.3	19.8	(11.0)	(32.0)	22.5	38.0
Omo L40-19 Max	306.0	247.0	253.0	13.0	13.5	20.1	17.1	10.0	20.2	28.2	27.1	29.1	(25.0)	16.3	19.8	(12.0)	(35.0)	22.5	38.0
SKX 8761					13.0	14.0			18.0	23.0	21.0	22.0	14.0	17.0	14.0	10.0	25.0	19.0	26.0
STW 113					15.0	16.0			19.0	27.0	21.0	24.0	20.0	14.0	18.0	12.0	32.0	22.0	41.0
STW 380					15.0	15.0			17.0	21.0	21.0	22.0	19.0	15.0	16.0	10.0	29.0	18.0	32.0
STW 398									16.0	22.0	16.0	18.0	16.0	12.0	16.0	9.0	27.0		21.0
STW 432a					15.0	15.0			18.0	28.0	21.0	26.0		12.0	19.0			21.0	40.0
TM 1517e									17.0		19.0	22.0		14.0	15.0				

[1] The Omo L40-19 ulna is missing three measurements due to damage on the coronoid process (TrocCord, TrocSt, CorHt). In the discriminant function analyses, these measurements were replaced by maximum and minimum measurements consistent with the preserved morphology. The estimated measurements are given in parentheses, and Omo L40-19 is entered into the analyses as two specimens, one with the maximum inferred measurements (Omo L40-19 Max) and one with the minimum inferred measurements (Omo L40-19 min). All measurements were taken on original specimens except for Omo L40-19, where the measurements were taken on the cast from the Natural History Museum, London.

variation are assessed by the average taxonomic distance, which is calculated as the square root of the mean sum of the squares of the differences between the values for n characters between two individuals. Shape differences, independent of size, are based on the size-corrected average taxonomic distance. This is calculated in the same way as the average taxonomic distance, except that the values for each variable are divided by the geometric mean of all the variables for that specimen.

Previous probability-oriented analyses of taxon variation in hominin paleontology have assumed the null hypothesis that the specimens are conspecific (Martin and Andrews, 1984, 1993; Kimbel and White, 1988; Wood et al., 1991; Kramer, 1993; Thackeray, 1997). However, the overlap between the ranges of intraspecific variation and interspecific variation can be considerable (Aiello et al., unpublished results), so that it is advisable to test the alternative hypothesis, that the specimens belong to different species. These two tests allow for the accurate assessment of both type I and type II error (Sokal and Rohlf, 1981).

In order to achieve maximum separation and minimum overlap between the ranges of variation in the comparative sample, the measurements employed in the bootstrapping analyses should be chosen and/or weighted to maximize the variation between taxa and minimize the variation within those taxa. This is particularly important for bones such as the ulna, where taxonomically and/or functionally significant intertaxon differences may be subtle in relation to substantial similarities in size and shape. Discriminant function analysis is designed to achieve this end (Tabachnick and Fidell, 1989). Thus, the bootstrapping analyses presented here are based not on raw (or on size-corrected raw) data, but on scores from discriminant function analyses of the raw and size-corrected data. The specific techniques employed will be described fully.

RESULTS AND DISCUSSION

Reconstruction of OH 36

The analyses performed to reconstruct the length of OH 36 were carried out using the sample of modern humans and African apes

TABLE 3. List of measurements and definitions[1]

1. Length to head: maximum length of the olecranon process to the distal articular surface, measured along the shaft axis (M1, McH1) (Length).	*0.57* (0.4)
2. Length to the pronator quadratus crest: Maximum length from the proximal point of the olecranon process to the most proximal point of the pronator quadratus crest (PQlength).	*1.12* (1.8)
3. Curvature cord: maximum distance between the point of inflection opposite the tip of the coronoid process and the point of minimum distal circumference (maximum dorsal concavity) (ETp) (CurvCord).[2]	*1.25* (2.3)
4. Curvature subtense: maximum subtense from the chord (+ is convex) (ETp) (CurvSt).[2]	*0.34* (10.3)
5. Crest, minimum breadth: breadth of the shaft perpendicular to the maximum development of the interosseous crest (CrestMin).[2]	*0.10* (2.6)
6. Crest, maximum breadth: breadth of the shaft taken at the point of maximum development of the interosseous crest (CrestMax).[2]	*0.23* (4.3)
7. Maximum breadth of the pronator quadratus crest: maximum breadth across the most projecting portion of the pronator quadratus crest (ETp) (PQMax).[2]	*0.35* (8.3)
8. Minimum breadth of the pronator quadratus crest: breadth taken perpendicular to the maximum breadth (ETp) (PQMin).[2]	*0.15* (2.2)
9. Olecranon length: distance from the middle of the trochlear notch to the proximal point on the olecranon process (M8, McH12, S8) (OlecLt).[2]	*0.27* (3.1)
10. Olecranon height: anteroposterior length of the olecranon process (M7, McH9, S6) (OlecHt).[2]	*0.25* (2.0)
11. Olecranon breadth (articular): maximum mediolateral breadth of the olecranon process across the joint surface (M6) (OlecArt).[2]	*0.14* (0.8)
12. Olecranon breadth (maximum): maximum mediolateral breadth across the whole of the olecranon process (M6) (OlecMax). Note that for some ulnae, this measurement may be identical to no. 11 (OlecArt).[2]	*0.17* (1.2)
13. Trochlear length: minimum distance between the anterior projections of the olecranon and coronoid processes, measured along the mid-trochlear ridge (M7(1), McH10) (TrocCord).[2]	*0.26* (1.8)
14. Trochlear transverse width: minimum width, in the transverse plane, of the trochlear notch taken perpendicular to the shaft axis (McH6) (TrocTv).[2]	*0.20* (2.3)
15. Trochlear antero-posterior height: minimum distance between the floor of the trochlear notch on the posterior surface (McH7, S2) (TrocAp).[2]	*0.20* (2.8)
16. Trochlear notch subtense: maximum distance from the trochlear notch chord to the deepest point on the mid-notch ridge (S4) (TrocSt).[2]	*0.10* (1.6)
17. Coronoid height: maximum anteroposterior distance from the posterior surface to the anterior surface of the coronoid process (McH8, S3) (CorHt).[2]	*0.21* (1.3)
18. Coronoid breadth: breadth of the lower sigmoid notch (F4) (CorBt).[2]	*0.50* (2.8)
19. Position of tuberosity: distance between the middle of the trochlear notch and the middle of the tuberosity, taken parallel to the shaft axis (McH11) (PosTub).[2]	*0.79* (4.3)
20. Computed measurement: (OlecDif) = difference between the olecranon maximum breadth (OlecMax) and the olecranon articular breadth (OlecArt).[2]	n.a.
21. Computed measurement: (CorHtDif) = difference between the height of the coronoid (CorHt) and the height of the olecranon (OlecHt).[2]	n.a.

[1] Results of an investigation of interobserver error using the Andaman Island sample (n = 10) are given in the final column. Figures in italics are percentage prediction errors, and figures in parentheses are coefficients of variation. Codes in parentheses after the measurement definitions refer to author and measurement number in published references. ETp, Erik Trinkaus, personal communication; F, Feldesman (1979); M, Martin (1928); McH, McHenry et al. (1976); S, Senut (1981).
[2] Measurements used in the discriminant function and bootstrapping analyses.

given in Table 1. The longest measurement that can be determined directly on OH 36 is the distance from the proximal surface of the olecranon to the proximal margin of the pronator quadratus crest (PQlength). This measurement is strongly correlated with overall ulnar length (Length) in each of the three genus-based comparative samples (modern human, chimpanzee, and gorilla; orangutans were not included in this analysis) and also in the combined modern human and African ape sample (Table 4). However, the length to the pronator quadratus crest is not significantly correlated with distal ulnar length (DULength: the distance from the proximal margin of the pronator quadratus crest to the most distal point on the ulnar head) in modern humans and gorillas. The two measurements correlate relatively poorly, but nonetheless significantly, in the chimpanzee sample and in the combined modern human and African ape samples (Table 4).

In order to accurately predict overall ulnar length, the predictor variable, or variables, should have a high correlation, not with total bone length, but with the length of the distal part of the ulna (DULength). Stepwise multiple regression analyses (using SPSS for Windows release 7.5.1) based on raw data showed that different combinations of independent variables were the best

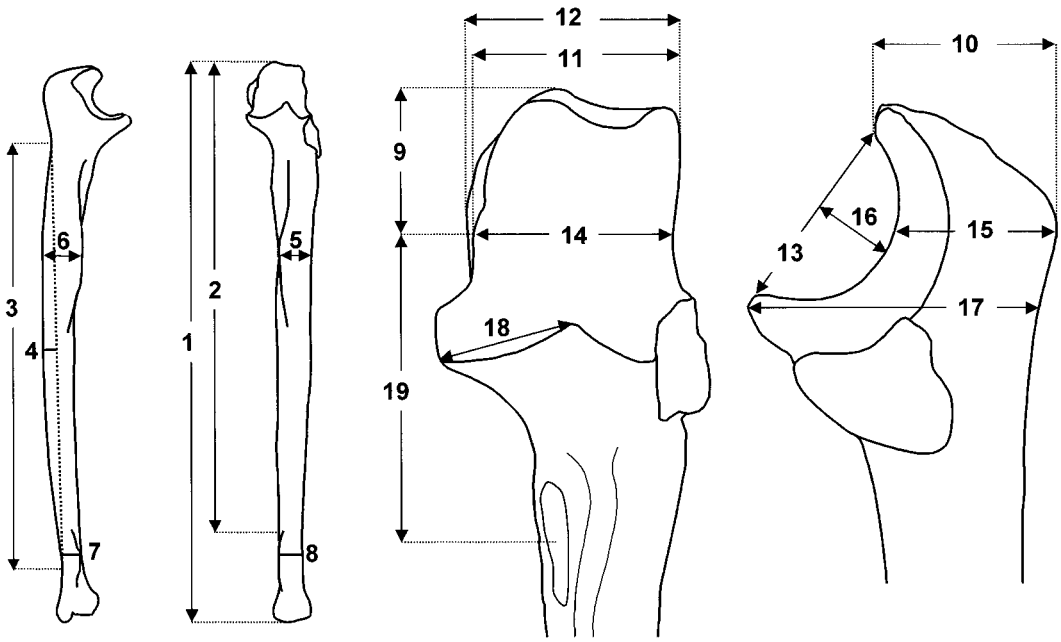

Fig. 2. Ulnar measurements used in this analysis. See Table 3 for description of measurements. Numbers refer to measurement numbers in Table 3.

TABLE 4. Ulnar length correlations for the three genus-based comparative samples (Homo, Pan, and Gorilla) and for the combined modern human and African ape sample[1]

Variables	Total sample	*Homo*	*Pan*	*Gorilla*
Length vs. DULength	0.27*	−0.04	−0.34*	0.29
Length vs. PQLength	0.97*	0.88*	0.75*	0.98*

[1] DULength, distance from the proximal margin of the pronator quadratus crest to the most distal point on the ulnar head.
* $P < 0.05$.

predictor variables for distal ulnar length in each of the comparative samples (modern humans, gorillas, and chimpanzees) and in the combined African ape and human sample (Table 5). Multiple correlations ranged from 0.69 ($r^2 = 0.48$) in the gorilla sample to 0.96 ($r^2 = 0.93$) for the chimpanzee sample. The equations based on the individual comparative samples and on the combined African Ape and human sample resulted in different predicted total lengths for the OH 36 ulna. Using chimpanzees as a reference sample, the length of that part of OH 36 which is distal to the proximal edge of the pronator quadratus crest was estimated to be 41.2 mm (standard error = 2.9); this resulted in a predicted total ulnar length of 274 mm (Table 5). This is 6 mm shorter than would be predicted on the basis of the modern human comparative sample, and almost 30 mm shorter than the length predicted on the basis of the gorilla sample.

The length of the KNM-BK 66 ulna was inferred in the same fashion. It also showed a discrepancy between the predicted length based on the gorilla sample (299 mm) and that based on the modern human sample (284 mm). It should be noted that the shortest predicted length for the Baringo ulna in the present analysis (284 mm) is still 11 mm longer than the length of 273 mm reported by Solan and Day (1992). These authors used minimum shaft diameter as their predictor variable, but did not report the strength of the correlation between this variable and total ulnar length. Solan and Day (1992) concluded from comparisons based on modern humans that the shaft of KNM-BK 66 was elongated in relation to the size of its proximal joint surface. Based on the current analysis, it is probable that KNM-BK 66 is relatively even more elongated than these authors suggest. The accu-

TABLE 5. Multiple regression equations and ulnar length predictions for OH 36, KNM-BK 66, and OMO L40-19[1]

Variables	Total sample	*Homo*	*Pan*	*Gorilla*
Equations for the prediction of ulnar length based on the various reference populations				
CrestMin	0.82	1.34		
CurvCord	0.49	0.76	0.85	
CurvSt			−0.54	
OlecDif				2.58
OlecLt	1.00	1.00		
PosTub	0.48			
PQLength	−0.60	−0.84	−0.81	
PQMin	0.78			1.53
PQMax			1.18	
TrocCord			0.69	
TrocSt	−1.27			
Constant	37.70	32.67	19.47	38.45
Coefficient of determination and standard error				
r^2	0.65	0.77	0.93	0.48
Standard error	6.92	5.56	2.92	6.79
Predicted ulnar lengths (mm)				
OH 36				
DULength	53	47	41	70
Length	286	280	274	303
KNM-BK 66				
DULength	43	39	45	54
Length	288	284	290	299
OMO L40-19				
DULength	58	56	60	59
Length	305	303	307	306

[1]Multiple regression equations predict the length of the ulna distal to the pronator quadratus crest (DULength). To determine DULength based on the total sample or any one of the three genus-based comparative samples, multiply the value in the appropriate column by the measurement for the corresponding variable and sum across all variables. Total length of the ulna is determined by adding the predicted DULength to the length of the ulna to the pronator quadratus crest (PQLength) (see Table 2). Key to the variable acronyms is given in Table 3.

racy of the multiple regression equations was tested on the complete Omo L40-19 ulna that has an overall length (to the head) of 306 mm (Howell and Wood, 1974). Predicted lengths for this fossil ulna based on all four comparative samples (modern humans, chimpanzees, gorillas, and the combined modern human and African ape sample) are very close to the known total length (Table 5).

Which of the comparative samples provides the most suitable model for reconstructing the length of the OH 36 ulna? Anticipating the results of the discriminant function analyses, which are set out below, OH 36 is consistently most similar to the chimpanzees and then to modern humans in its overall morphology. It is therefore probable that the actual length of OH 36 would have been closer to that predicted on the basis of the chimpanzee (274 mm) or the modern human comparative sample (280 mm), rather than to the greater length (303 mm) which results if the prediction is based on the gorilla sample.

Comparative morphological and functional assessment

To provide an appropriate framework for the analysis of the fossil hominin ulnae, discriminant function analyses were carried out to assess the similarities and differences in ulnar morphology within the modern comparative samples, and between the modern comparative samples and the fossil ulnae. The 19 ulnar measurements from Table 3 were used as predictors of membership in four groups, modern humans (n = 142), chimpanzees (n = 52; *P. paniscus* and both subspecies of *P. troglodytes* were pooled), gorillas (n = 32), and fossil hominins (n = 4). In Omo L40-19, three (TrocCord, TrocSt, CorHt) of the 19 measurements used in the analysis are missing. These were replaced by the minimum and the maximum anatomically consistent measurements, based on an assessment of the preserved morphology. Thus, two versions of Omo L40-19 were entered into the analyses, one with the minimum values for the missing measurements (Omo Min), and one with the maximum values (Omo Max).

Two sets of analyses were carried out, one on the raw data (reflecting both size and shape) and one on size-corrected data (emphasizing shape). The data do not violate the assumptions of linearity, normality, multicollinearity, or singularity which underlie multivariate analysis. Both sets of analyses resulted in four significant discriminant functions (Table 6). The first discriminated between humans and the apes, the second between chimpanzees and the remaining apes, the third between orangutans and the other comparators, and the fourth between the fossil ulnae and the comparators (Table 6, Figs. 3, 4).

The pattern of correlations of the predictor measurements with the discriminant

TABLE 6. Results of discriminant function analyses

Function	Eigenvalue	% of variance	Cumulative %	Canonical correlation
Analysis based on raw data				
1	8.33	59.4	59.4	0.95
2	3.31	23.6	83.0	0.88
3	1.97	14.0	97.0	0.81
4	0.42	3.0	100.0	0.54
Analysis based on size-corrected data				
1	4.85	53.8	53.8	0.91
2	2.44	27.1	81.0	0.84
3	1.36	15.0	96.0	0.76
4	0.36	4.0	100.0	0.51

functions in both of the discriminant function analyses (raw and size-corrected data) suggests that humans have absolutely and relatively less curved ulnae than the apes (Table 7, discriminant function 1 for both analyses). Human ulnae also have an absolutely shorter and narrower trochlea (TrocCord, TrocTv), less buttressing posterior to the trochlea (TrocAp), and narrower and shorter shafts (CrestMax, PQMax, PQMin, CurvCord). Relative to overall size, however, the shaft of the human ulna is robust (CrestMax, PQMax, PQMin). It is also large proximally, with a relatively long and deep trochlea (TrocCord, TrocSt), a relatively long olecranon process (OlecLt), and a relatively wide and high coronoid process (CorTv, CorAp). The functional significance of some of these relative relationships may be confounded by the fact that humans have relatively short ulnae in relation to body mass (Aiello and Dean, 1990). This is because ulnar length is an absolutely much larger measurement than the others used in the computation of the geometric mean (Table 1), and thus will have a disproportionate influence on it.

Chimpanzees, in both absolute and relative terms, have coronoid and olecranon processes of more similar height than do the other apes (CorHtDiff) (Table 7, discriminant function 2 for both sets of analyses). They have absolutely shorter and narrower olecranon processes (OlecLt, OlecArt, OlecMax), a narrower coronoid process (CorTv), and a shallower trochlea (TrocSt). Relative to size, the chimpanzee olecranon is tall (OlecHt), and the trochlea is narrow (TrocTv).

Orangutans have absolutely shorter olecranon and coronoid heights (OlecHt, CorAp) than do the other comparators (Table 7, discriminant function 3 for both sets of

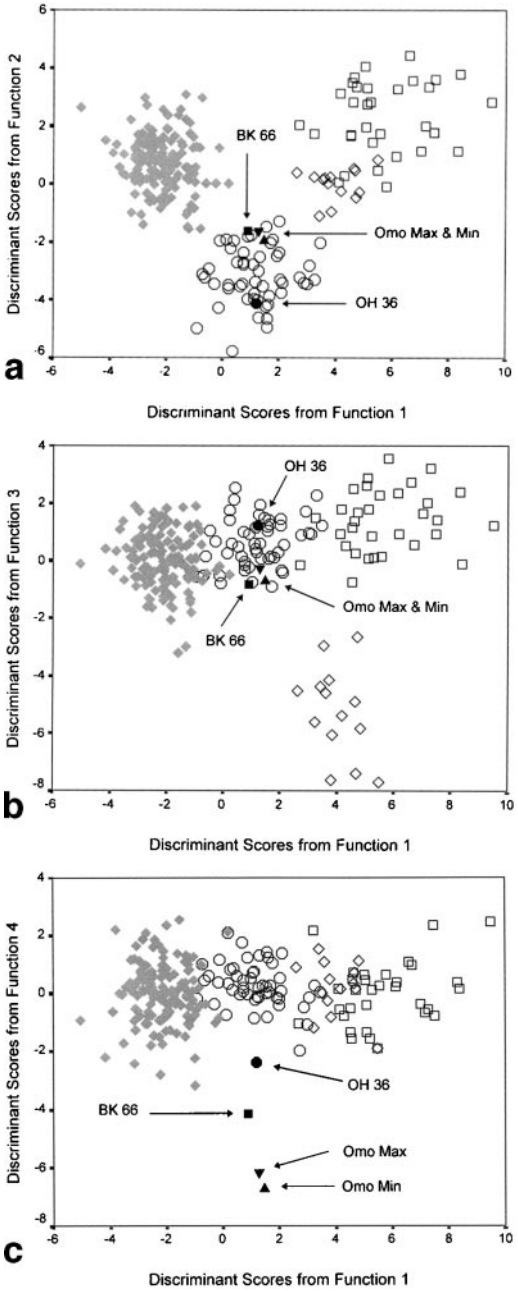

Fig. 3. Discriminant function plots for the analysis of raw data (size and shape). Discriminant Scores from Function 1 are plotted against those from Function 2 (**a**), from Function 3 (**b**), and from Function 4 (**c**). Humans, gray diamonds; *Gorilla*, open squares; *Pan*, open circles; *Pongo*, open diamonds; OH 36, solid circles; KNM-BK 66, solid squares; Omo L40-19 Min, upward triangle; Omo L40-19 Max, downward triangle. Correlations of predictor variables with the discriminant functions are given in Table 7.

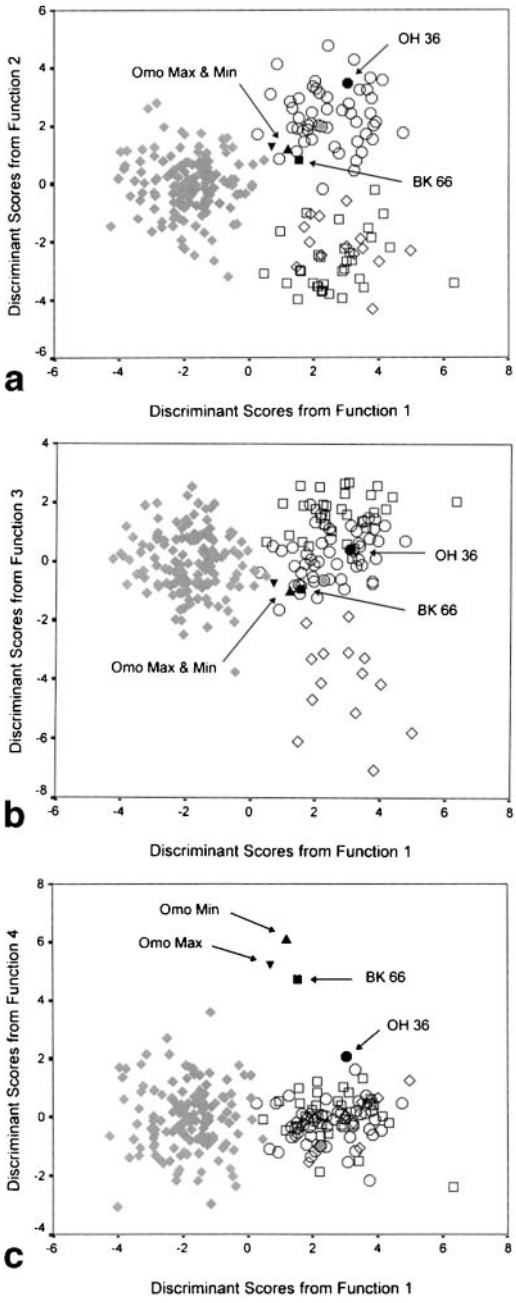

Fig. 4. Discriminant function plots for the analysis of size-corrected data (reflecting shape). Discriminant scores from Function 1 are plotted against those from Function 2 (**a**), from Function 3 (**b**), and from Function 4 (**c**). Symbols as in Figure 3. Correlations of predictor variables with the discriminant functions are given in Table 7.

analyses). Relative to size, however, they are distinguished by longer ulnae (CurvCord) and a more distally situated ulnar tuberosity (PosTub). The fossils are distinguished from the remaining sample by absolutely large maximum widths of the pronator crest (PQMax) and relatively small minimum diameters of the ulnar crest (CrestMin) (Table 7, discriminant function 4 for both sets of analyses).

The features that distinguish the great majority of humans from the apes on the first discriminant function (raw data reflecting both size and shape) are most probably linked with the differences in relative muscularity of the forearms in humans and apes. In particular, the greater distance between the floor of the trochlea and the dorsal surface of the shaft (TrocAp) in the apes strengthens and buttresses the proximal ulna at its narrowest point posterior to the trochlea, and the greater difference between the articular breadth and total breadth of the olecranon (OlecDif) reflects both overall strength and an increased area for muscle attachment.

Can any of these features be interpreted in the context of the role the ulna plays in providing support during quadrupedal terrestrial locomotion in chimpanzees and gorillas? It has been argued that a weight-supporting ulna should have an anteroproximally-oriented trochlea to provide a "cradle" to support the humerus when the arm is fully extended (Fischer, 1906; Kapandji, 1982; Aiello and Dean, 1990). It has also been argued that the coronoid in quadrupeds should be wide and heavily buttressed (Knussman, 1967). This analysis provides no support for either of these hypotheses. The orientation of the trochlea, as reflected in the difference in height between the coronoid and the olecranon, loads on the second discriminant function in both the raw data and size-corrected analyses, but this discriminant function separates chimpanzees from gorillas and orangutans, not modern humans and the apes (Table 7). A plot of the difference between the height of the coronoid and the height of the olecranon (CorHtDif) demonstrates the gradation from a predominantly anteriorly oriented trochlea in chimpanzees, through the intermediate condition in modern humans, to the anteroproximally

TABLE 7. Correlations of predictor variables with discriminant functions[1]

	Analysis based on raw data (function)					Analysis based on size-corrected data (function)			
	1	2	3	4		1	2	3	4
TrocTv	.594[2]	.478	.278	.004	CurvSt	.594[2]	.206	.026	.026
CurvSt	.576[2]	−.349	.176	−.019	OlecArt	−.383[2]	−.091	.085	.035
CurvCord	.517[2]	.001	−.235	−.050	TrocSt	−.382[2]	.091	−.079	−.146
PosTub	.422[2]	.196	−.199	−.032	OlecMax	−.369[2]	−.074	.121	.066
TrocAp	.406[2]	.048	.383	.049	PQMax	−.365[2]	.065	−.090	.279
CrestMin	.357[2]	.178	.165	−.071	CorHt	−.329[2]	.090	.068	−.214
CrestMax	.274[2]	.238	.220	−.121	OlecLt	−.329[2]	.089	−.045	−.083
TrocCord	.265[2]	.235	.071	−.023	TrocCord	−.299[2]	.008	−.142	−.035
PQMin	.197[2]	.134	.189	.046	PQMin	−.289[2]	.107	−.009	−.148
CorHtDif	.128	.468[2]	.022	.196	OlecDif	.284[2]	.123	.081	.094
OlecArt	.242	.453[2]	.309	−.138	CorTv	−.246[2]	−.161	−.104	−.226
OlecMax	.243	.397[2]	.340	−.083	CrestMax	−.213[2]	−.016	.005	.012
CorTv	.332	.388[2]	.075	.158	TrocAp	−.114[2]	.081	.062	−.104
TrocSt	.208	.305[2]	.171	−.017	TrocTv	.041	−.382[2]	.139	−.010
OlecLt	.205	.262[2]	.223	.002	OlecHt	−.151	.351[2]	.083	−.061
OlecHt	.246	−.115	.357[2]	−.039	CorHtDif	−.303	−.345[2]	−.008	−.249
CorHt	.303	.232	.324[2]	.105	CurvCord	−.064	.094	−.414[2]	−.053
OlecDif	.053	−.094	.166[2]	.158	PostTub	−.087	−.099	−.383[2]	−.044
PQMax	.171	.220	.135	−.428[2]	CrestMin	−.049	−.011	−.011	−.180[2]

[1]Pooled within-groups correlations between discriminating variables and standardized canonical discriminant functions. Variables are ordered by absolute size of correlation within each function.
[2]Largest absolute correlation between each variable and any discriminant function.

oriented trochlea in gorillas (Fig. 5a). The same pattern is true if trochlear orientation is measured by the coronoid height index (coronoid height/olecranon height · 100). These results suggest that, as in modern humans, the differences in the orientation of the trochlea among the African ape samples may be related to differences in the habitual position of loading (Trinkaus and Churchill, 1988). Within the apes, factors other than weight support in terrestrial locomotion would seem to be major determinants of trochlear orientation (Inouye, 1997). In relation to relative size of the trochlea, a plot of the trochlear index (trochlear transverse diameter/trochlear cord · 100) also shows that modern humans and chimpanzees (both *P. paniscus* and *P. troglodytes*) are similar, while gorillas and orangutans are distinguished by having a relatively wide trochlea (Fig. 5b).

Fossil hominin ulnae

The discriminant analyses, based on either the raw or the size-corrected data, were effective at correctly classifying individual ulnae in the comparative groups. The raw data analysis correctly classified 99% of the original cases, incorrectly classifying only two ulnae, one human ulna, and the OH 36 ulna, as chimpanzees. The size-corrected analysis correctly classified 98% of the original cases. One human ulna was misclassified as an orangutan and another as a fossil; once again, OH 36 was incorrectly classified as a chimpanzee. None of the fossil hominin ulnae were confused with orangutan ulnae (see also Figs. 3, 4).

Bivariate comparisons using the variables that scored highly in the discriminant function analyses permit an assessment of the taxonomic affinities of the less complete fossil Plio-Pleistocene hominin ulnae in relation to each other, to the more complete OH 36, KNM-BK 66, and Omo L40-19 hominin ulnae, and to the comparative extant hominoid sample. In these analyses OH 36 is the most chimpanzee-like on the basis of those measurements that distinguish the apes from modern humans, and from each other (Fig. 6a, b). These include the considerable buttressing posterior to the trochlea (TrocAp) (Fig. 6a), and the height of the olecranon which increases the attachment area and improves the leverage of triceps (Fig. 6b). These features, together with the markedly keeled trochlea, would suggest that the OH 36 elbow had considerable strength and stability throughout the full range of flexion and extension. In addition, the pronator crest is wide relative to the curvature cord (Fig. 6c), suggesting that the pronator qua-

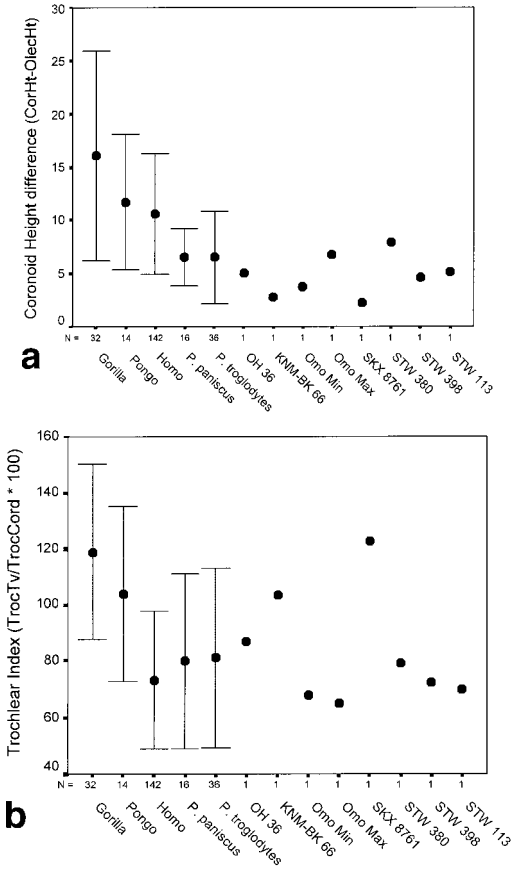

Fig. 5. **a:** Difference in height of the coronoid and olecranon processes (CorHt-OlecHt) in the comparative sample and selected fossil hominins. **b:** Trochlear index (TrocTv/TrocCord · 100) in the comparative sample and selected fossil hominins. Solid circles, means; error bars, 2 standard deviations.

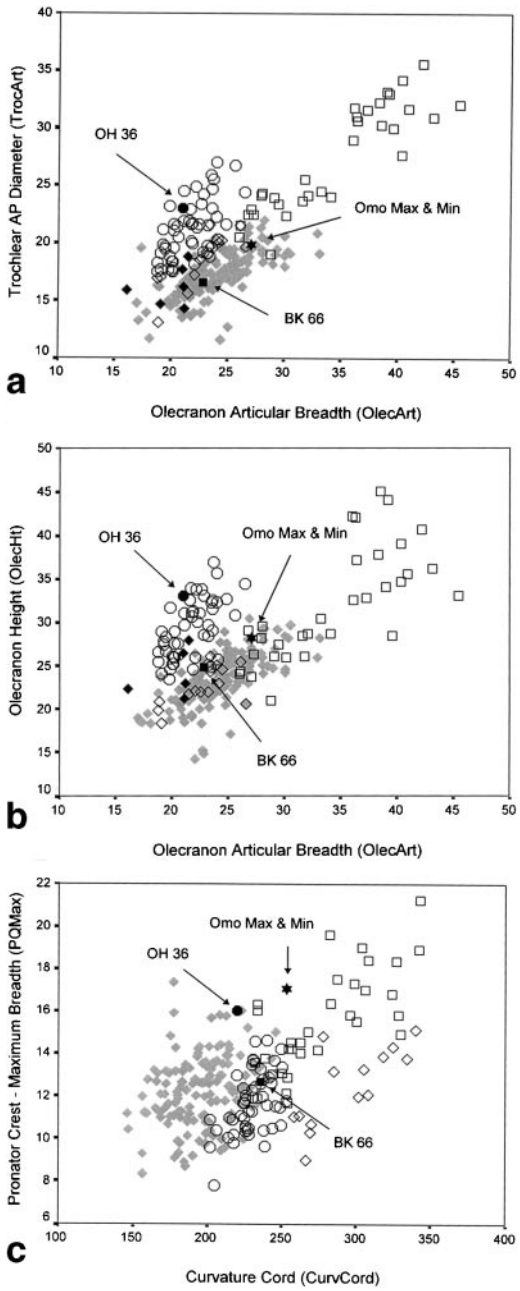

Fig. 6. **a:** Bivariate plot of olecranon articular breadth (OlecArt) and trochlear anterior-posterior diameter (TrocAp). **b:** Bivariate plot of olecranon articular breadth and olecranon height (OlecHt). **c:** Bivariate plot of the curvature cord (curvcord) and the maximum breadth of the pronator crest (PQMax). Solid diamonds, Southern African fossil hominins (see Table 2). Other symbols as in Figure 3.

dratus was well-developed. This feature is shared with Omo L40-19.

Although OH 36 resembles chimpanzees in features that reflect forearm strength, one qualitative feature of OH 36 suggests that this individual did not support its weight on its forelimbs when moving on the ground. All of the chimpanzee and gorilla ulnae examined for this study have a medially-projecting olecranon (Fig. 7), which places insertion of the triceps brachii medial to the long axis of the trochlea. This feature is absent in the orangutan, and thus it is most likely related to the more terrestrial habitus of the extant African ape. In modern humans, the insertion for the triceps is more symmetrically orientated so that it is in line

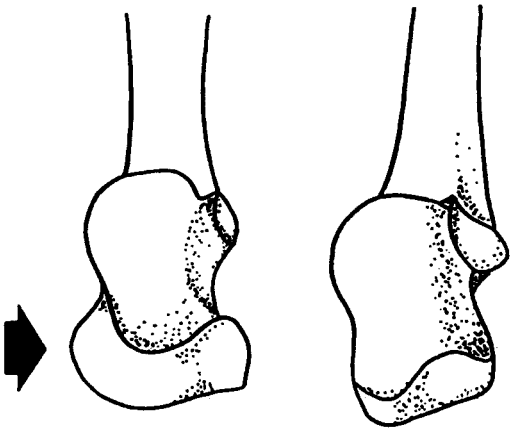

Fig. 7. Diagram of the right proximal ulna of (left) *Pan* and (right) *Homo.* Arrow indicates the medially projecting olecranon in *Pan.*

with the axis of the trochlea. The vertical lateral wall of the olecranon fossa has long been recognized as part of a locking mechanism of the weight-supporting elbow, but to our knowledge the case for the association of this feature of the ulna with terrestriality has not previously been made. The OH 36 olecranon lacks the African ape-like medial projection, and at least in this respect aligns itself with the other fossil hominin ulnae and with the modern human sample.

The main conclusion that can be drawn from these comparisons is that the Olduvai ulna comes from an individual with more powerful forearms than are found in living humans, or in many of the other fossil hominin ulnae. The marked shaft curvature of OH 36 is consistent with this interpretation. The tall olecranon, the buttressed trochlea, and the mediolateral extension of the olecranon beyond the articular surface would have served to increase the insertion area of the triceps brachii and would have provided strength and support to the elbow joint. The keeled trochlea would have stabilized the elbow joint throughout the range of flexion and extension.

Taxonomic assessment of OH36

The probability that OH 36 was a member of the same species as either KNM-BK 66 or Omo L40-19 was assessed using bootstrapping techniques based on the discriminant function scores derived from the preceding analyses. The modern human and ape comparative samples show a substantial range of intra- and interspecific variation. The "single-species" hypothesis should be rejected if the difference between OH 36 and either of the other two fossil ulnae is greater than would be expected on the basis of intraspecific variation in modern humans and modern apes. Bootstrapping was carried out by drawing 1,000 samples of n = 2 from each of three of the four modern comparator groups (humans, gorillas, and chimpanzees; the sample size for the orangutans was too small), thereby providing an empirical basis for assessing the probability that the variation seen in any pair of fossil hominin ulnae would exceed that expected in any one of the modern comparator groups. Bootstrapping was similarly carried out to determine the range of variation expected in intertaxon comparisons. One thousand repeated samples were drawn, where each of the pair of ulnae came from one of the following combinations of comparator groups: human-chimpanzee, human-gorilla, and chimpanzee-gorilla. These provided the empirical basis for assessing the probability that the variation seen in any pair of fossil ulnae would be of the degree expected in two ulnae belonging to taxa as different in ulnar size, morphology, and/or function as the three comparator pairings. As described in Materials and Methods, size differences were assessed using the geometric mean (GM) of all 19 measurements for each individual. Combined size and shape differences were based on discriminant function scores derived from the previous analysis of raw data. All four significant discriminant function scores were used in each analysis and were analyzed on the basis of average taxonomic distance. Shape differences were based on discriminant function scores derived from analysis of size-corrected data. Discriminant function scores were used in preference to actual measurements in order to maximize interspecific differences and minimize intraspecific differences (see Materials and Methods).

In the analysis of size differences, as assessed by the ratio of the geometric means, there was considerable overlap between the size dimorphism that would be expected

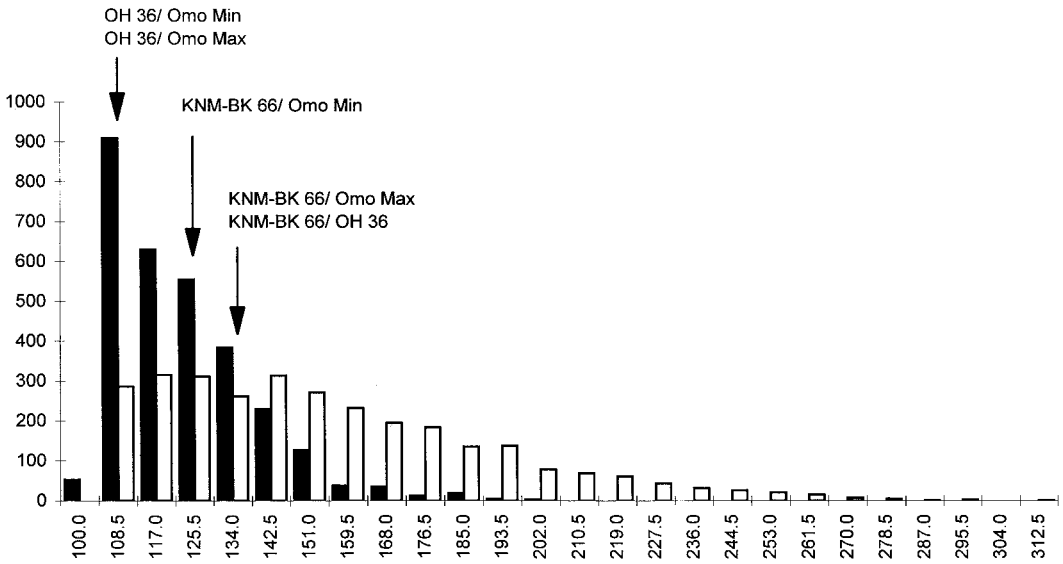

Fig. 8. Bootstrapped comparisons based on size differences. Size difference is based on the ratio of geometric means. Solid bars represent intrataxon comparisons, and open bars intertaxon comparisons.

within each of the comparator taxa and that observed between the comparator pairings (Fig. 8). KNM-BK 66, with a geometric mean of 15.0, is considerably smaller than either OH 36 (GM = 19.7) or Omo L40-19 (GM for Omo Min = 18.5, and for Omo Max = 19.3). With one exception, the size dimorphism observed in any of the fossil pairings was insignificantly different from the range of variation expected either intraspecifically in the comparative samples, or interspecifically (Table 8). The exception was the size similarity between OH 36 and Omo L40-19 (both Omo Max and Omo Min). These pairings were significantly more similar ($P < 0.05$) than would be expected if they derived from two taxa as different in size as modern humans and gorillas. The OH 36 pairing with Omo Min was also significantly more similar in size than would be expected in an interspecific chimpanzee and gorilla pairing, or in a pooled interspecific analysis based on the combined interspecific differences observed in the comparators (humans, chimpanzees, and gorillas).

There was, however, considerable and significant difference in shape in each of the fossil ulna pairings. OH 36 and Omo L40-19 (both Max and Min) were consistently more different in shape than would be expected in any of the three intrataxon comparators, or in the pooled intrataxon sample (Fig. 9, Table 8). At the same time, the OH 36/Omo L40-19 pairing was not significantly different from the degree of shape difference that would be expected between any of the three comparator taxa (human/chimpanzee, human/gorilla, and gorilla/chimpanzee), or in the pooled intertaxon sample. This analysis supports the hypothesis that OH 36 and Omo L40-19 came from separate taxa that differed in forearm function to the degree found between the modern comparator pairings. Suggestions that OH 36 should be referred to the same taxon as Omo L40-19 (Walker and Leakey, 1993) may have been primarily influenced by the similar size of these two fossil ulnae.

The results of the OH36/Omo L40-19 comparison contrast with the finding that KNM-BK 66 and Omo L40-19 (both Max and Min) were consistently as similar in shape as any two ulnae drawn from the three intrataxon comparators (humans, chimpanzees, or gorillas), or from the pooled intrataxon sample (Fig. 9, Table 8), and were significantly more similar in shape than would be expected in any of the intertaxon

TABLE 8. Bootstrapping probabilities[1]

Value for fossil pair	Intrataxon analyses				Intertaxon analyses			
	Gorilla	*Homo*	*Pan*	Pooled intrataxon	*Homo/Gorilla*	*Homo/Pan*	*Pan/Gorilla*	Pooled intertaxon
OH 36/Omo Min (Omo Max)								
106.20 (104.3), size dimorphism	0.73 (0.79)	0.80 (0.87)	0.72 (0.80)	0.75 (0.82)	0.02* (0.01)*	0.14 (0.01)	0.06 (0.03)*	0.07 (0.05)*
2.62 (2.39), size and shape	0.06 (0.11)	0.01* (0.02)*	0.00* (0.01)*	0.02* (0.05)*	0.02* (0.01)*	0.39 (0.26)	0.10 (0.06)	0.17 (0.11)
2.59 (2.33), shape only	0.01* (0.04)*	0.02* (0.04)*	0.00* (0.01)*	0.01* (0.03)*	0.27 (0.15)	0.40 (0.26)	0.31 (0.19)	0.33 (0.20)
OH 36/KNM-BK 66								
131.60, size dimorphism	0.23	0.22	0.10	0.18	0.13	0.66	0.33	0.37
1.86, size and shape	0.33	0.12	0.60	0.17	0.00*	0.70	0.01*	0.03*
2.13, shape only	0.06	0.07	0.02*	0.05*	0.09	0.17	0.13	0.13
KNM-BK 66/Omo Min (Omo Max)								
123.80 (129.20), size dimorphism	0.37 (0.27)	0.38 (0.27)	0.20 (0.12)	0.33 (0.22)	0.07 (0.11)	0.55 (0.63)	0.25 (0.30)	0.29 (0.35)
1.34 (1.07), size and shape	0.67 (0.83)	0.43 (0.62)	0.34 (0.56)	0.48 (0.67)	0.00* (0.00)*	0.02* (0.00)*	0.00* (0.00)*	0.01* (0.00)*
0.71 (0.56), shape only	0.84 (0.91)	0.91 (0.96)	0.85 (0.93)	0.86 (0.93)	0.00* (0.00)*	0.00* (0.00)*	0.00* (0.00)*	0.00* (0.00)*

[1] Bootstrapping analyses are calculated on the basis of the 19 variables indicated in Table 3. Bootstrapping was carried out by drawing 1,000 repeated samples of n = 2 from each of three modern comparator groups (humans, chimpanzees, and gorillas) and from each of three modern intertaxon groups (*Homo/Pan, Homo/Gorilla,* and *Pan/Gorilla*). The pooled intrataxon sample was composed of the pooled results of the three intrataxon analyses (n = 3,000), and the pooled intertaxon sample was composed of the pooled results of the intertaxon analyses (n = 3,000). For intrataxon analyses, probabilities are the proportion of pairs with values greater than that found in the fossil comparison. For intertaxon analyses, probabilities are the proportion of pairs with values less than those found in the fossil comparison. Values for the fossil comparison are given in the first column. In parentheses are values for Omo Max.

*$P < 0.05$.

comparisons, or in the pooled intertaxon sample. This result is unexpected in view of the fact that Omo L40-19 is usually attributed to *P. boisei*, whereas KNM-BK 66 is widely regarded as belonging to *Homo erectus* (Senut, 1981; Solan and Day, 1992; Wood, in press), with marked similarities to later archaic *H. sapiens* ulnae (Churchill et al., 1996; Pearson and Grine, 1996). The differences between Omo L40-19 and KNM-BK 66 have more to do with overall differences in size than to functionally significant differences in shape.

The interpretation of differences and similarities in shape was more ambiguous for the pairing between OH 36 and KNM-BK 66. The shape difference observed in this pairing was significantly greater than the intrataxon differences observed in chimpanzees ($P = 0.019$) and in the pooled intrataxon sample ($P = 0.046$) (Fig. 9, Table 8). The shape difference would, however, be compatible with levels of intrataxon differences observed in gorillas ($P = 0.057$), in humans ($P = 0.066$), and in all of the intertaxon comparisons.

For the pairings between OH 36 and Omo L40-19, and between KNM-BK 66 and Omo L40-19, bootstrapping based on raw data (reflecting both size and shape) produced results that are fully consistent with the shape-based analysis (Table 8). However, the results were different for OH 36 and KNM-BK 66 (Fig. 10, Table 8). The size and shape differences between these two fossils were consistent with those in each of the intrataxon comparators and in the pooled intrataxon sample, but the differences between the fossil pairing were significantly less than those in the intertaxon comparisons between humans and gorillas ($P = 0.003$) and between chimpanzees and gorillas ($P = 0.014$), and in the pooled intrataxon sample ($P = 0.030$).

Thus, on shape alone, the differences between OH 36 and KNM-BK 66 are similar to those between the intertaxon pairings, yet they are consistent with the level of variation within taxa when the comparisons are based on both size and shape. This may be due to the fact that similarities and differences based solely on size (ratio of geometric means) and those based on both size and

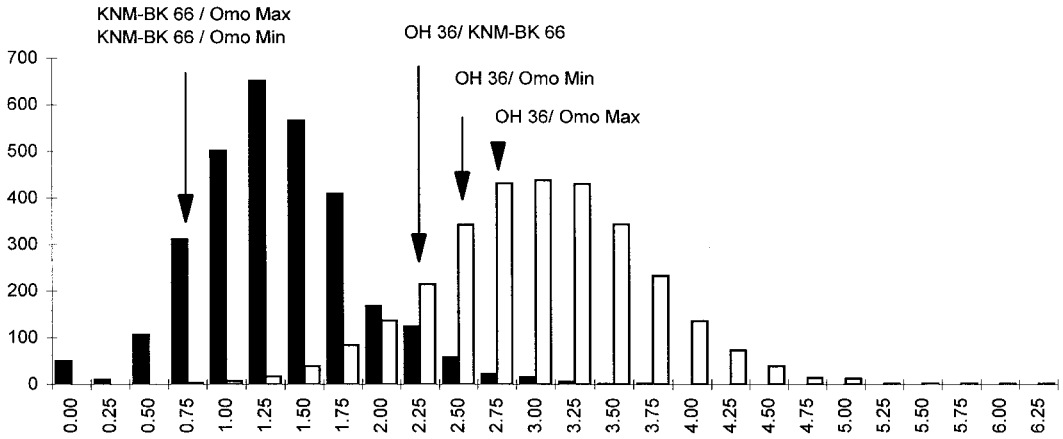

Fig. 9. Bootstrapped comparisons based on average taxonomic distance (size-corrected data), reflecting shape variation within and between taxa. Solid bars represent intrataxon comparisons, and open bars intertaxon comparisons.

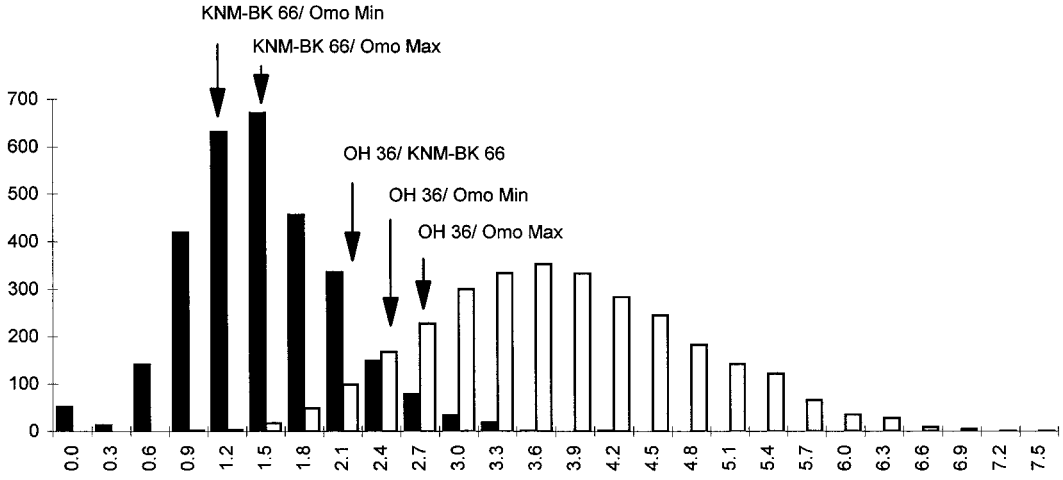

Fig. 10. Bootstrapped comparisons based on average taxonomic distance (nonsize-corrected data), reflecting both size and shape variation within and between taxa. Solid bars represent intrataxon comparisons, and open bars intertaxon comparisons.

shape (average taxonomic distances based on raw data) are more strongly correlated with each other than either is with similarities and differences based on shape alone (average taxonomic distances based on size-corrected data) (Richmond and Jungers, 1995). For example, there are much greater differences in both size dimorphism and combined size and shape dimorphism in the human/gorilla and chimpanzee/gorilla intertaxon comparisons than there is in the human/chimpanzee intertaxon comparison (Table 9). The fact that size dimorphism in the fossil pairing (=131.6) is considerably less than the mean for the human/gorilla (mean = 176.4, SD = 37.8) and less than the chimpanzee/gorilla (mean = 146.1, SD = 27.4) intertaxon comparisons most probably contributes to the significance of the intertaxon size and shape comparisons. Furthermore, the fact that the single-taxon hypothesis for the pairing between OH 36 and Omo L40-19 can be so strongly rejected on the basis of both the shape, and the size

TABLE 9. Dimorphism in the intertaxon comparisons

	Mean	Standard deviation
Size dimorphism		
Homo/Pan	126.2	19.6
Homo/Gorilla	176.4	37.8
Pan/Gorilla	146.1	27.4
Size and shape dimorphism		
Homo/Pan	9.9	5.3
Homo/Gorilla	21.9	9.4
Pan/Gorilla	15.6	8.0
Shape dimorphism		
Homo/Pan	0.6	0.3
Homo/Gorilla	0.8	0.4
Pan/Gorilla	0.6	0.3

and shape analyses, and that for the pairing between KNM-BK 66 and Omo L40-19 the hypothesis can be so strongly accepted, suggests that the single-taxon hypothesis for OH 36 and KNM-BK 66 can be rejected.

CONCLUSIONS

This comparative study has demonstrated that OH 36 is significantly different from the early hominin ulna, Omo L40-19, recovered from the Shungura Formation, and that OH 36 is also most probably significantly different from the Middle Pleistocene ulna recovered from the Baringo Formation, KNM-BK 66. Given these results, is it possible to assign any of these hominin ulnae to their appropriate taxa?

The three fossil hominin ulnae all come from East Africa, a region which for much of the past 2.5 Myr has supported two, or more, synchronic hominin taxa (Wood, 1996) (Fig. 12). One of the three ulnae, OH 36, comes from a time period (Fig. 12), and a site, at which there is evidence of at least two synchronic hominin taxa, *P. boisei* and *H. erectus* (Leakey LSB, 1961; Leakey MD, 1978). The second, Omo L40-19, is from Member E of the Omo Shungura Formation and is dated to c. 2.3 Myr (Feibel et al., 1989). The fossil record from the Shungura Formation during this time period also apparently samples two fossil hominins, *P. boisei,* and *Homo* sp. (Howell et al., 1987), or aff. *Homo* sp. indet. (Suwa et al., 1996). The remains of early African *H. erectus,* or *H. ergaster,* have been recovered from nearby sites in the Omo region. The oldest of these, at Koobi Fora, dates from c. 1.9 Myr (Feibel et al., 1989; Wood, in press, 1999) (Fig. 12), but this first appearance date (FAD) may be an artifact, for no immediately older sediments are preserved in this part of the Omo region. The third of the three ulnae, KNM-BK 66, also comes from a time period in which there is a strong possibility that at least two hominin taxa were regionally sympatric (Wood, in press) (Fig. 12). The two species, *H. erectus* and *Homo heidelbergensis,* are both securely attributed to the genus *Homo,* and thus there is every expectation that the forelimb morphology of both taxa would have closely resembled that of modern humans. Moreover, the nature of the hominin mandibular remains found in the Kapthurin Formation suggests that the hominin sampled there is more likely to have been *H. erectus* than *H. heidelbergensis* (Wood, in press, 1999). Thus, any exploration of the taxonomy of these three ulnae should sensibly start from the provisional assumption that KNM-BK 66 samples *H. erectus* (Senut, 1981; Solan and Day, 1992; Churchill et al., 1996; Pearson and Grine, 1996; Wood, in press, 1999).

Turning to OH 36, there is good evidence to suggest that two hominin species, *H. erectus* and *P. boisei,* are known from Upper Bed II at Olduvai, the former represented by OH 9, and the latter by OH 3 and 38 (Howell, 1978; Wood et al., 1994). It would be parsimonious to assume that OH 36 represented one, or the other, of these taxa, and on the basis of the evidence presented here, it is unlikely that OH 36 represents *H. erectus.* Among the clearest contrasts between OH 36 and KNM-BK 66, the former has a markedly curved shaft and a substantial supinator crest, and if OH 36 was attributed to *H. erectus,* then this taxon would have an extraordinarily high level of intraspecific variability (Table 8, Fig. 9). Alternatively, could OH 36 belong instead to early African *H. erectus,* or *H. ergaster?* The first associated skeleton of that taxon to be recovered was KNM-ER 803. Its femoral morphology was interpreted as linking it with the *Homo* clade (Day, 1976; McHenry et al., 1976; Howell, 1978). A substantial length of the shaft of the left ulna (KNM-ER 803 C) is preserved (Day and Leakey, 1974), and although its supinator crest is described as "prominent" (Day and Leakey, 1974, p 369), it is a good deal less well-developed than

that of OH 36, and there is no evidence of the degree of shaft curvature (Day and Leakey, 1974, Plate 3, p 377) that is seen in OH 36. The best-preserved postcranial material incontrovertibly linked with early African *H. erectus,* or *H. ergaster,* belongs to the juvenile associated skeleton KNM-WT 15000 (Walker and Leakey, 1993). Both ulnae of KNM-WT 15000 (BP and BZ) are complete except for their epiphyses, and both have much straighter shafts than OH 36 (Walker and Leakey, p 132–135). Therefore, the evidence of straight ulna shafts from both KNM-ER 803 and KNM-WT 15000 suggests that it is improbable that OH 36 belongs to early African *H. erectus* or *H. ergaster.*

If allocation to early African *H. erectus* or *H. ergaster* is inappropriate, is there any evidence to link OH 36 with *P. boisei,* the only other hominin taxon known from that time at Olduvai Gorge? There is only one associated skeleton potentially linked to *P. boisei,* and that is KNM-ER 1500. Grausz et al. (1988) allocated it to *P. boisei* on the basis of a fragment, KNM-ER 1500 (O), of the base of the right side of the mandible. However, Wood (1991) concluded that the mandible fragment is too fragmentary to allocate at the specific level with any degree of confidence. In any event, the proximal end (F) and the fragment of the shaft (I) of the right ulna of KNM-ER 1500 are too fragmentary to help with taxonomic discrimination at the species level. Nonetheless, despite the lack of a securely attributed associated skeleton of *P. boisei,* the morphology of OH 36 is consistent in both size and morphological similarity to the large, robust humerus from Koobi Fora, KNM-ER 739. For example, the latter has a distal articular morphology that is compatible with the marked keeling of the trochlea of OH 36. Lague and Jungers (1996) challenged the attribution of KNM-ER 739 to *P. boisei,* and instead suggested that it be attributed to *Homo rudolfensis.* They explain that their suggestion is "based mainly on current craniodental attributions" (Lague and Jungers, 1996, p 425), but the KNM-ER 739 humerus postdates the most recent craniodental evidence for *H. rudolfensis* by approximately half a million years. What is clear, however, is that if OH 36 is allocated to *P. boisei,* then along with the dental evidence from equivalent-aged horizons at Olduvai, it represents, at least for the time being, the most recent evidence for *P. boisei.*

Lastly, what can be said about the taxonomy of the Shungura ulna, Omo L40-19? The many significant differences between it and OH 36, and the significant similarity between it and the presumed *H. erectus* ulna, KNM-BK 66, pose interesting interpretative problems. Could the previous allocation of Omo L40-19 to *P. boisei* (Howell and Wood, 1974) be incorrect? Could it belong to another taxon? Although teeth from Member E of the Shungura Formation have been assigned to *Homo* sp., there is no evidence that they belong to *H. erectus.* Suwa et al. (1996) undertook a detailed analysis of this dental evidence, and although they concluded that the teeth belong to *Homo,* and that they are closer in morphology to *H. rudolfensis* than to *H. habilis,* they refrained from allocating them to *H. rudolfensis* because they suggested that the differences between the the latter taxon and *H. habilis* could be due to anagenetic evolution within a single taxon. As has been noted above, the remains of early African *H. erectus* or *H. ergaster* have been recovered from sites nearby within the Omo region. The earliest evidence for this taxon may be as old as c. 1.9 Myr (Feibel et al., 1989; Wood, 1991), and the disconformity immediately beneath this horizon opens the possibility that early African *H. erectus,* or *H. ergaster,* may be closer in age to the hominins from Member E of the Shungura Formation than the FAD suggests. The overall morphological similarity of Omo L40-19 to KNM-BK 66, e.g., shaft curvature in relation to overall length (curvature cord) (Fig. 11), would certainly support the allocation of Omo L40-19 to a taxon with a later *Homo*-like forelimb morphology. At present it is not possible to tell whether Omo L40-19 provides the earliest evidence of early African *H. erectus* or *H. ergaster,* or whether it represents fossil evidence of the forearm of *H. rudolfensis* or *H. habilis.*

If the latter were the case, however, the large size of the Shungura ulna would imply that a representative of one, or the other, of these two taxa was either large overall, or that it had relatively long forearms. The

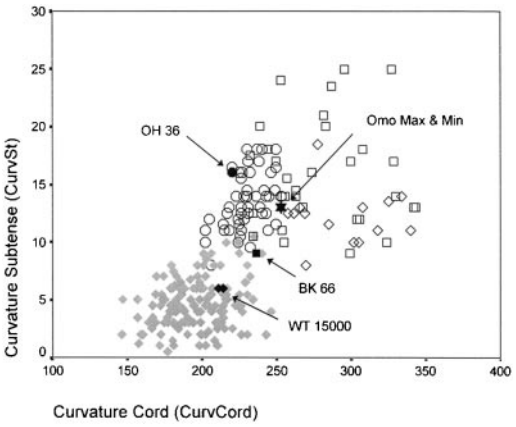

Fig. 11. Bivariate plot of the curvature cord (CurvCord) against the curvature subtense (CurvSt). Note the magnitude of shaft curvature in OH 36 in relation to the other fossil hominins. All measurements in millimeters. Symbols as in Figure 3. Solid diamonds, KNM-WT 15000, left and right sides.

large body size would be inconsistent with current estimates of the body mass of *H. habilis* based on the OH 62 skeleton (Hartwig-Scherer and Martin, 1991), but would be consistent with cranially derived estimates of the body mass of *H. rudolfensis* (Aiello and Wood, 1994). If Omo 40-19 did transpire to belong to *H. rudolfensis*, this would have profound implications for our understanding of the adaptive grade of the earliest representatives of the genus *Homo* (Wood and Collard, in press, 1999).

A further possibility is that the Shungura ulna does represent *Paranthropus*, and that the latter taxon shows considerable temporal variation in the morphology and inferred function of the forearm. However, this would not be consistent with other evidence for morphological stasis in *P. boisei* (Wood et al., 1994), and it would mean that the aspects of ulna shape that are shared by Omo L40-19 and later *Homo* would have to be viewed as

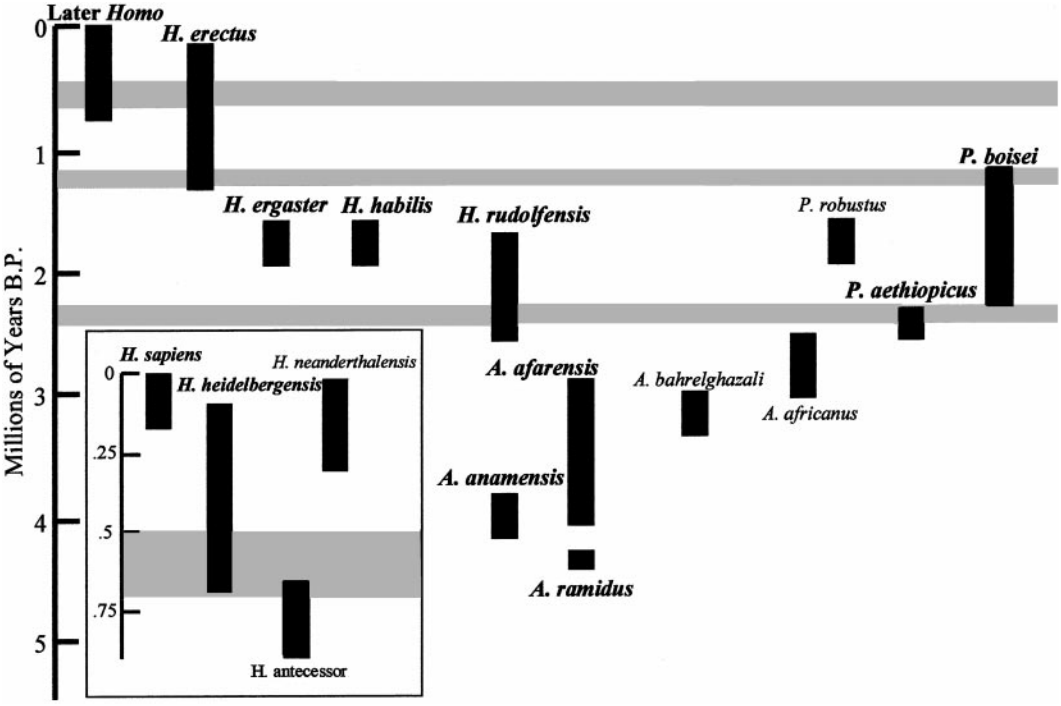

Fig. 12. Plot of time ranges of hominin species, with the East African taxa in bold type. The approximate time ranges of the three best-preserved hominin ulnae are shown as three horizontal gray bands. The topmost band is for KNM-BK 66, the middle for OH 36, and the lowermost for Omo L40-19. The single band within the box is for KNM-BK 66.

either synapomorphies, or primitive retentions. Until we have a much better understanding of the evolution of the hominin postcranium, we suggest a more cautious approach to the taxonomy of Omo L40-19, and that it be allocated to the tribe Hominini gen. et sp. indet. for the time being.

In conclusion, the evidence available points to the probability that OH 36 and KNM-BK 66 belong to different hominin species, and the likelihood that OH 36 belongs to *P. boisei*. In functional terms, the OH 36 ulna belonged to an individual with relatively powerful forearms and a musculature that would have provided strength and support to the elbow joint throughout the full range of flexion and extension. This, as well as overall multivariate similarities with the chimpanzees, would be consistent with a locomotor repertoire that included at least some arboreal climbing behavior. The similarities between KNM-BK 66 and Omo L40-19 make the initial allocation of this ulna to *P. boisei* (Howell and Wood, 1974) much less certain. The results of this study remind us about how little we know about the evolution of the hominin postcranium and locomotion in the Plio-Pleistocene.

ACKNOWLEDGMENTS

We are grateful to Theya Molleson and Robert Kruzynski for access to the material held in the Natural History Museum, London, and also to the curatorial staff at the Canadian Museum of Civilization, Ottawa, and at the Musée royal de l'Afrique centrale, Tervuren, Belgium. The fossil hominins were studied at the National Museum of Kenya and at the Department of Anatomy, University of Witwatersrand, Johannesburg, South Africa. We thank Emma Mbua at the former, and Phillip Tobias, Ron Clarke, and Lee Berger at the latter, for their assistance. We are grateful to the ultimate custodians of the fossils for their permission to carry out this study. We thank Mike Rose, Brian Richmond, Mark Collard, and an anonymous referee for valuable and constructive criticism of an earlier draft of this manuscript. Our research was supported by grants from the Leverhulme Trust to L.C.A. (F 134 BB) and B.W. (A 953767). B.W. was also supported by the Henry R. Luce Foundation.

LITERATURE CITED

Aiello LC, Dean MC. 1990. An introduction to human evolutionary anatomy. London: Academic Press.

Aiello LC, Wood BA. 1994. Cranial variables as predictors of hominine body mass. Am J Phys Anthropol 95:409–426.

Carney J, Hill A, Miller JA, Walker A. 1971. Late australopithecine from Baringo district, Kenya. Nature 230:509–514.

Churchill SE, Pearson OM, Grine FE, Trinkaus E, Holliday TW. 1996. Morphological affinities of the proximal ulna from Klasies River main site: archaic or modern? J Hum Evol 31:213–237.

Day MH. 1976. Hominid postcranial remains from the East Rudolf Succession. In: Coppens Y, Howell FC, Isaac GLL, Leakey REF, editors. Earliest man and environments in the Lake Rudolf Basin. Chicago: University of Chicago Press. p 507–521.

Day MH. 1986. Guide to fossil man, 4th ed. London: Cassell. p 1–432.

Day MH, Leakey REF. 1974. New evidence of the genus *Homo* from East Rudolf, Kenya (III). Am J Phys Anthropol 41:367–380.

Feibel CS, Brown FH, McDougall I. 1989. Stratigraphic context of fossil hominids from the Omo group deposits: Northern Turkana Basin, Kenya, and Ethiopia. Am J Phys Anthropol 78:595–622.

Feldesman MR. 1979. Further morphometric studies of the ulna from the Omo Basin, Ethiopia. Am J Phys Anthropol 51:409–416.

Fischer E. 1906. Die Variationen am Radius und Ulna des Menschen. Z Morphol Anthropol 9:147–247.

Gowlett JAJ, Harris JWK, Walton D, Wood BA. 1981. Early archaeological sites, hominid remains and traces of fire from Chesowanja, Kenya. Nature 294:125–129.

Grausz HM, Leakey REF, Walker AC, Ward CV. 1988. Associated cranial and postcranial bones of *Australopithecus boisei*. In: Grine FE, editor. Evolutionary history of the "robust" australopithecines. New York: Aldine de Gruyter. p 127–132.

Grine FE, Demes B, Jungers WL, Cole TM III. 1993. Taxonomic affinity of the early *Homo* cranium from Swartkrans, South Africa. Am J Phys Anthropol 92: 411–426.

Grine FE, Jungers WL, Schultz J. 1996. Phenetic affinities among early *Homo* crania from East and South Africa. J Hum Evol 30:189–225.

Hartwig-Scherer S, Martin RD. 1991. Was Lucy more human than her child—observations on early hominid postcranial skeletons. J Hum Evol 21:439–449.

Hay RL. 1976. Geology of the Olduvai Gorge. Berkeley: University of California Press. p 1–203.

Howell FC. 1978. Hominidae. In: Maglio VJ, Cooke HBS, editors. Evolution of African mammals. Cambridge: Harvard University Press. p 154–248.

Howell FC, Wood BA. 1974. Early hominid ulna from the Omo Basin, Ethiopia. Nature 249:174–176.

Howell FC, Haesaerts P, de Heinzelin J. 1987. Depositional environments, archeological occurrences and hominids from Members E and F of the Shungura Formation (Omo Basin, Ethiopia). J Hum Evol 16:665–700.

Inouye S. 1997. Functional implications of elbow morphology for knuckle-walking in juvenile and adult African apes. Am J Phys Anthropol [Suppl] 24:135 (abstract).

Kapandji IA. 1982. The physiology of the joints. Volume 1: upper limb, 5th ed. Edinburgh: Churchill Livingstone. p 1–204.

Kimbel WH, White TD. 1988. Variation, sexual dimorphism and the taxonomy of *Australopithecus.* In: Grine FE, editor. Evolutionary history of the "robust" australopithecines. New York: Aldine de Gruyter. p 175–192.

Knussman R. 1967. Humerus, Ulna and Radius der Simiae. Bibl. Primatol., volume 5. Basel: S. Karger. 399 p.

Kramer A. 1993. Human taxonomic diversity in the Pleistocene: does *Homo erectus* represent multiple hominid species? Am J Phys Anthropol 91:161–171.

Kramer A, Donnelly SM, Kidder JH, Ousley SD, Olah SM. 1995. Craniometric variation in large-bodied hominoids: testing the single-species hypothesis for *Homo habilis.* J Hum Evol 29:443–462.

Lague MR, Jungers WL. 1996. Morphometric variation in Plio-Pleistocene hominid distal humeri. Am J Phys Anthropol 101:401–427.

Leakey LSB. 1961. New finds at Olduvai Gorge. Nature 189:649–650.

Leakey MD. 1978. Olduvai fossil hominids: their stratigraphic positions and associations. In: Jolly CJ, editor. Early hominids of Africa. London: Duckworth. p 3–16.

Lockwood CA, Richmond BG, Jungers WL, Kimbel WH. 1996. Randomization procedures and sexual dimorphism in *Australopithecus afarensis.* J Hum Evol 31:537–548.

Martin LB, Andrews P. 1984. The phyletic position of *Graecopithecus freybergi* Koenigswald. Cour Forsch Inst Senckenberg 69:25–40.

Martin LB, Andrews P. 1993. Species recognition in Middle Miocene hominoids. In Kimbel WH, Martin LB, editors. Species, species concepts and primate evolution. New York: Plenum Press. p 393–427.

McHenry HM, Corruccini RS, Howell FC. 1976. Analysis of an early hominid ulna from the Omo Basin, Ethiopia. Am J Phys Anthropol 44:295–304.

Pearson OM, Grine FE. 1996. Morphology of the Border Cave hominid ulna and humerus. S Afr J Sci 92:231–236.

Richmond BG, Jungers WL. 1995. Size variation and sexual dimorphism in *Australopithecus afarensis* and living hominoids. J Hum Evol 29:229–245.

Richmond BG, Jungers WL, Cole TM. 1993. Size and shape differences in the proximal femur of *Australopithecus afarensis:* two sexes, or two species? Am J Phys Anthropol [Suppl] 16:166 (abstract).

Rightmire GP. 1979. Cranial remains from *Homo erectus* from Beds II and IV, Olduvai Gorge, Tanzania. Am J Phys Anthropol 51:99–116.

Senut B. 1981. L'humérus et ses articulations chez les hominidés plio-pléistocènes. Cahiers de Paléontologie (Paléoanthropologie). Paris: Éditions du Centre Nacional de la Recherche Scientifique.

Sokal RR, Rohlf FJ. 1981. Biometry: the principles and practice of statistics in biological research. New York: W.H. Freeman. p 1–859.

Solan M, Day MH. 1992. The Baringo (Kapthurin) ulna. J Hum Evol 22:307–313.

Suwa G, White TD, Howell FC. 1996. Mandibular postcanine dentition from the Shungura Formation, Ethiopia: crown morphology, taxonomic allocations, and Plio-Pleistocene hominid evolution. Am J Phys Anthropol 101:247–282.

Tabachnick BG, Fidell LS. 1989. Using multivariate statistics, 2nd ed. New York: Harper Collins Publishers, Inc. p 1–746.

Thackeray JF. 1997. Probabilities of conspecificity. Nature 390:30–31.

Tobias PV. 1991. Olduvai Gorge: volume 4. The skulls, endocasts and teeth of *Homo habilis.* Cambridge: Cambridge University Press. p 1–921.

Trinkaus E. 1983. The Shanidar Neanderthals. New York: Academic Press. p 1–502.

Trinkaus E. 1989. Neandertal upper limb morphology and manipulation. In: Giacobini G, editor. Hominidae. Turin: Jaca Books. p 331–338.

Trinkaus E. 1992. Morphological contrasts between the Near Eastern Qafzeh-Skhul and late archaic human samples: grounds for a behavioral difference? In: Akazawa T, Aoki K, Kimura T, editors. The evolution and dispersal of modern humans in Asia. Tokyo: Hokusen-sha. p 277–294.

Trinkaus E, Churchill SE. 1988. Neanderthal radial tuberosity orientation. Am J Phys Anthropol 75: 15–21.

Walker A, Leakey R. 1993. The Nariokotome *Homo erectus* skeleton. Cambridge: Harvard University Press. p 1–457.

Wood BA. 1991. Koobi Fora research project. Volume 4. Hominid cranial remains. Oxford: Clarendon Press. p 1–466.

Wood BA. 1996. Human evolution. Bioessays 18:945–954.

Wood BA. In press. 1999. Plio-Pleistocene hominins from the Baringo Region, Kenya. Proc Geol Soc.

Wood BA, Collard M. In press 1999. Rethinking the genus *Homo.* Science.

Wood BA, Li Y, Willoughby C. 1991. Intraspecific variation and sexual dimorphism in cranial and dental variables among higher primates and their bearing on the hominid fossil record. J Hum Evol 174:185–205.

Wood BA, Wood CW, Konigsberg L. 1994. *Paranthropus biosei*—an example of evolutionary stasis? Am J Phys Anthropol 95:117–136.